PET Measures of Amphetamine-Induced Dopamine Release in Ventral versus Dorsal Striatum

Wayne C. Drevets, M.D., Julie C. Price, Ph.D., David J. Kupfer, M.D., Paul E. Kinahan, Ph.D., Brian Lopresti, B.S., Daniel Holt, B.S., and Chester Mathis, Ph.D.

Regional differences in dextroamphetamine (AMPH)-induced dopamine (DA) release in the baboon striatum were assessed using positron emission tomographic (PET) measures of [^{11}C]raclopride specific binding to DA D2/D3 receptors acquired before and after AMPH administration. The magnitude of the reduction in [^{11}C]raclopride binding, following AMPH administration, was two-fold greater in the anteroventral striatum (comprised of ventral caudate, anteroventral putamen, and nucleus accumbens) than the dorsal striatum (dorsal caudate). A simulation study demonstrated that any potential biases due to resolution (partial volume) and alignment effects were significantly smaller than the magnitude of the observed results. These regional differences in the sensitivity to AMPH are compatible with microdialysis evidence in rats indicating that the magnitude of DA release in response to AMPH concentrations in the range tested is greater in ventral than dorsal striatal regions. Post hoc tests involving measures in other striatal regions showed that the baseline DA D2/D3 binding was highest and the correlation between AMPH dose and change in [^{11}C]raclopride binding most significant in the putamen. [**Neuropsychopharmacology 21:694–709, 1999**]   © 1999 American College of Neuropsychopharmacology. Published by Elsevier Science Inc.

The release of cerebral dopamine (DA) in response to pharmacological and behavioral challenges can be noninvasively measured by functional neuroimaging assessments of the competition between DA and radiolabelled DA receptor ligands for binding to DA receptors. The most sensitive of these techniques uses PET to measure changes in the binding potential (BP) of the DA D2/D3-receptor antagonist [^{11}C]raclopride. The sensi-

tivity of [^{11}C]raclopride binding to competition from endogenous DA is at least partly conferred by raclopride's relatively fast dissociation rate and low affinity for DA D2 receptors (K_D = 1.2 nM) (Seeman et al. 1989; Kohler et al. 1985). The striatal BP for [^{11}C]raclopride has thus been shown to decrease following administration of drugs that stimulate DA release (e.g., AMPH) or block DA reuptake (e.g., methylphenidate, cocaine) and during performance of neuropsychological tasks presumed to increase DA release (Breier et al. 1997; Carson et al. 1997; Dewey et al. 1993; Hartvig et al. 1997; Koepp et al. 1998; Laruelle et al. 1996, 1997; Price et al. 1998; Schlaepfer et al. 1997; Volkow et al. 1994).

Neuroimaging measures of *in vivo* DA release are expected to yield seminal information regarding the pathophysiology of psychiatric conditions that have been associated with altered dopaminergic function, such as psychotic disorders, substance dependence dis-

NEUROPSYCHOPHARMACOLOGY 1999–VOL. 21, NO. 6
© 1999 American College of Neuropsychopharmacology
Published by Elsevier Science Inc.
655 Avenue of the Americas, New York, NY 10010

0893-133X/99/$–see front matter
PII S0893-133X(99)00079-2

orders, and mood disorders (Breier et al. 1997; Fibiger 1991; Grace 1991; Laruelle et al. 1996; Schlaepfer et al. 1997; Swerdlow & Koob 1987; Volkow et al. 1994; Willner 1995). The system of primary interest in these conditions involves the mesocorticolimbic dopaminergic projections from the ventral tegmental area and substantia nigra into the ventral striatum, medial prefrontal cortex, and amygdala, which participate in the neural processing of motivated behavior (Everitt et al. 1989; Fibiger 1991; Heimer and Alheid 1991; Willner et al. 1991). Alterations in this system are thus hypothesized to play roles in mediating the euphoria and behavioral reinforcement associated with drugs of abuse and mania as well as the anhedonia, inactivity and amotivation that characterize major depression (Deutch 1993; Fibiger 1991; Grace 1991; Swerdlow and Koob 1987; Willner 1995). The portion of this system where DA release is most clearly measurable by extant neuroimaging methods is the ventral striatum, since the specific-to-nonspecific binding ratio for the radiolabeled DA D2/D3 receptor radioligands that are sensitive to competition from DA is much higher in the D2/D3 receptor rich striatum than in the prefrontal cortex or the amygdala (Hall et al. 1994).

The ventral striatum may also comprise the striatal region where neuroimaging measures will demonstrate the greatest sensitivity to changes in radioligand binding induced by drugs that inhibit DA reuptake, stimulate DA release, or increase DA through neurotransmitter system interactions. This expectation follows from microdialysis studies in rats showing that higher extracellular fluid DA concentrations are achieved in the nucleus accumbens than the dorsal caudate-putamen during administration of cocaine, phencyclidine, nomiphensine, AMPH, nicotine, narcotic analgesics, and ethanol (Brazell et al. 1990; Carboni et al. 1989; Di Chiara and Imperato 1988a, b; Di Chiara et al. 1993; Imperato and Di Chiara 1986; Imperato et al. 1986; Kuczenski and Segal 1992; Segal and Kuczenski 1992; Sharp et al. 1987). In the case of AMPH, which stimulates release of cytosolic DA through a mechanism that is independent of DA neuronal firing activity (Kuczenski and Segal 1989), a preferential sensitivity of the accumbens to the DA releasing effects of AMPH was initially shown by Di Chiara and Imperato (1988b) and confirmed by some (Sharp et al. 1987) but not other studies (Robinson and Camp 1990; Pehek et al. 1990; Kuczenski and Segal 1992). The inconsistency of these results appeared to reflect differences in dialysis probe placement across studies. In fact, the ability to detect regional differences in AMPH sensitivity required that the dialysate from the dorsal caudate did not include extracellular fluid from the ventral striatum, and that the dialysate from the accumbens included fluid from the accumbens shell (DiChiara 1991; DiChiara et al. 1993). For example, Di-Chiara et al. (1993) found that ~two-fold greater in-

crease in extracellular fluid DA concentrations induced by AMPH (at all doses tested from 0.25 to 2.0 mg/kg) in the accumbens relative to the dorsal caudate-putamen was largely attributable to DA release in the shell, as opposed to the core, of the accumbens.

In primates, the accumbens cells blend with those of the anteroventral putamen and the ventral caudate, so that a distinct border of the accumbens shell is not microscopically or macroscopically evident (Heimer and Alheid 1991). Nevertheless, replication of the earlier microdialysis study of Di Chiara and Imperato (1988b), which used microdialysis probes positioned horizontally in two planes, one in dorsal caudate-putamen and the other in ventral striatum (traversing accumbens and anteroventral caudate-putamen), is technically feasible using neuroimaging techniques. Improvements in the spatial resolution of PET scanners and development of PET-MRI image coregistration methods permit close approximation of these probe positions using PET measures (Black et al. 1997).

The current study compares the magnitude of AMPH-induced changes in [11C]raclopride binding potential (ΔBP) in these two striatal regions in baboons to assess whether the differential sensitivity to AMPH between the anteroventral striatum and dorsal caudate seen in rodents also exists in primates. Because these structures are small relative to PET's spatial resolution, such quantitative neuroimaging assessments are subject to potential bias from the blurring associated with the scanner partial volume effects and from inaccuracies in the PET-MRI image coregistration. The influence of these error sources on our ability to test the hypothesis that the AMPH-induced ΔBP differs across striatal ROI is thus characterized by extending the previous simulation study of these effects in human brain imaging (Meltzer et al. in press) to the geometry of the baboon brain images presented here.

METHODS

PET Image Acquisition

Twelve paired [11C]raclopride PET studies were performed in five adult baboons (three female) in accordance with the Guide for the Care and Use of Laboratory Animals adopted by the NIH (Table 1). Each study consisted of a baseline [11C]raclopride scan followed 2 hours later by an identical scan that was preceded by AMPH administration. Prior to the baseline scan, the baboons were initially sedated with ketamine (20 mg/kg, i.m.), given atropine (1.0 mg, i.m.) to control salivation, and intubated. Anesthesia was subsequently maintained with isofluorane (0.5 to 2.5%, to effect) and paralysis with pancuronium (up to 0.06 mg/kg/hr, titrated to effect). At least 90 min elapsed between ketamine/atropine administration and image acquisition

to permit dissipation of any pharmacological effects of these agents on endogenous DA release prior to the baseline scan. During this period, a femoral artery catheter was inserted to monitor blood pressure and sample arterial blood, and an antecubital vein catheter was placed for radioligand infusion. Blood pressure, heart rate, and respiratory rate were monitored during the anesthesia and recovery periods. The baseline rectal body temperature (~37°C) was maintained using a Gaymar™ heating blanket. Prior to scanning, the baboon's head was fixed so that the image planes were acquired approximately parallel to the orbital-meatal line (Riche et al. 1988). This head position was maintained through both [^{11}C]raclopride scans.

Ten PET studies were performed using a Siemens 951R/31 (31 contiguous slices over a 108 mm axial field-of-view (FOV), and two using a Siemens HR+ (63 contiguous slices over a 152 mm axial FOV). When the HR+ became available toward the project end, scans were obtained on this tomograph because its superior sensitivity permitted injection of smaller injected masses of raclopride (Table 1). The slight differences in statistical noise and spatial resolution (described below in the Simulation Studies section) between the image sets acquired on each scanner were not expected to affect the quantitative accuracy of their respective mean ΔBP values.

A transmission scan was obtained to permit measured attenuation correction in all sessions using three ^{68}Ge/^{68}Ga rotating rod sources. High specific activity [^{11}C]raclopride (>1000 Ci/mmol) was synthesized as described by Halldin et al. (1991). Dynamic emission scans (20–25 frames of increasing length over 90 min) were initiated upon injection of [^{11}C]raclopride by slow i.v. bolus administration (over 30 sec). The administered dose of [^{11}C]raclopride ranged from 10 to 40 mCi for the 951R studies and 6 to 8 mCi for the HR+ studies (see Table 1 for injected mass). The 951R images were not corrected for scatter, as the 2D scatter fraction is ~10%. In contrast, the scatter fraction of the 3D HR+ images can approach ~40%, so these images were corrected using Siemens' model-based scatter correction method (Townsend et al. 1998). The PET images were filtered with a Hanning filter at the Nyquist frequency (reconstructed resolution described below).

The [^{11}C]raclopride input function was determined from arterial blood samples collected during the emission scan (35 total samples with 20 over the initial 2 min). Arterial blood was sampled at 2, 10, 30, 60, and 90 min post-injection to obtain the ratio of unmetabolized [^{11}C]raclopride to total plasma radioactivity using HPLC (Dewey et al. 1992). The time course of the fraction of unmetabolized [^{11}C]raclopride was fit to a sum of three exponentials and used to correct the total plasma radioactivity to obtain the input function (Price et al. 1998; Smith et al. 1998b).

About 120 min following the baseline [^{11}C]raclopride injection, AMPH was injected i.v. over 2 min and a second [^{11}C]raclopride injection was performed 5 min later, after initiating the AMPH pretreatment [in microdialysis studies of non-human primates the striatal DA concentration increases to a peak at 15–20 min post i.v. bolus injection of AMPH and remains elevated above baseline ≥60 min (Endres et al. 1997; Laruelle et

Table 1.   Characteristics of the Animals, the Time Intervals between AMPH Doses for Animals Studied on Multiple Days, the Injected Mass of Raclopride for Each Scan, and the Baseline BP Values

Baboon (gender)	Weight (kg)	Interval Between Studies (Weeks from Prior AMPH Exposure)[a]	AMPH Dose (mg/kg)	Injected Mass of Raclopride (nmol) Pre-AMPH Scan	Post-AMPH Scan	BP$_{Baseline}$ AVS	BP$_{Baseline}$ DCA
A (♀)	18	N/A	0.6	12.5	11.6	1.50	2.18
	18	60	0.3	1.4	1.5	1.90	2.29
	18	15	1.0	8.3	7.0	1.56	2.08
B (♂)	29	N/A	1.0	10.8	14.3	1.60	1.72
	29	31[b]	1.0	5.7	5.3	2.67	2.99
C (♂)	31	N/A	0.6	18.3	14.5	1.30	1.98
	31	64	0.3	3.5	2.0	1.32	1.88
	30	139	0.3	5.0	4.8	1.18	1.60
D (♀)	n.a.	N/A	0.6	21.4	19.5	0.95	1.67
	14	14	0.6	17.0	13.0	1.00	1.48
	14	89[b]	0.3	2.8	2.3	1.60	2.66
E (♀)	15	N/A	1.0	23.5	15.8	1.30	1.70

[a]The ΔBP values acquired in the same animals on subsequent dates did not reveal systematic order effects to suggest that sensitization had developed to the first or second AMPH administrations (e.g., among the animals imaged twice at the same AMPH dose, the second ΔBP value obtained was larger than the first for two animals and smaller for one. *Abbreviations*: n.a., not available.

[b]Indicates studies performed using a Siemens HR+ and the 3D image acquisition mode. All other scans were acquired in the 2D mode using a Siemens 951R.

al. 1997)]. The AMPH dose administered was 0.3 mg/ kg for four studies, 0.6 mg/kg for four, and 1.0 mg/kg for four (Table 1). Because of the concern that sensitization of DA neurons to the DA releasing effects of AMPH would bias dose response curves obtained within animals by increasing the DA response to subsequent administrations (Robinson and Kolb 1997), most animals were studied twice at the same dose to examine whether a time trend was evident in test-retest ΔBP measures, and only one animal underwent scan sessions at all three doses. Moreover, in animals studied more than once the AMPH exposures were separated by at least 12 weeks to avoid the development of sensitization (Robinson and Kolb 1997). For animals exposed to different AMPH doses the order of different doses was counterbalanced to reduce the likelihood that the development of sensitization would account for observed dose-response relationships.

MRI-Based Region-of-Interest (ROI) Definition

An MRI scan was obtained for each baboon using a 1.5 T GE Signa scanner and a 3-dimensional spoiled gradient recalled (SPGR) sequence (TE = 5, TR = 24, flip angle = 40°, slice thickness = 1.5 mm, NEX = 2, field of view = 12 mm, voxel size = 0.94 × 1.25 × 1.5 mm). This pulse sequence was optimized for delineating gray matter/white matter/CSF boundaries, facilitating the MRI-based ROI definition (Johnson et al.1993). In one animal, technical problems with the SPGR image precluded its use and a standard T1-weighted MRI image was used instead.

The post-AMPH PET image was aligned to the baseline PET image, and the MR image was aligned to the PET images and resliced to yield images in the same planes and with the same voxel size as the PET images. To facilitate coregistration, the brain was segmented from extrabrain tissues in the MR image using ANALYZE™ (Mayo Biomedical Engineering; Rochester, MN), and the MRI-PET alignment was performed using PET images comprised of the summation of frames from the first 15–30 min following [¹¹C]raclopride injection. This early distribution image overly represents free and nonspecifically bound tracer so that outlines of the cerebral and cerebellar cortex are sufficiently evident to guide image co-registration (Black et al. 1997; Woods et al. 1993).

The PET and MRI images were prepared for alignment by centering them at the mid-sagittal plane using the algorithm of Woods et al. (1993) and the method of Minoshima et al. (1992) for establishing symmetry (Wiseman et al. 1996). The centered images were then aligned using Automated Image Registration (AIR) (Woods et al. 1993). The precision of each PET-MR image alignment was verified in three dimensions using "iv_volumetool" software (C. Michel, University of

Louvain-la-Neuve, Belgium) by visually comparing seven internal points/ lines evident on both the PET and MRI images: the anterior and posterior most points of the corpus callosum, the midpoint of the thalamus, the basal and anterior borders of the temporal and frontal poles, and the basal and posterior surfaces of the occipital cortex (Wiseman et al. 1996).

Regions-of-interest (ROI) were defined on the aligned transverse MR image planes by manually tracing around the grey matter of that structure using Image-Tool™ (CTI PET Systems; Knoxville, TN) (Figure 1). The ROI defined in the 951R images were a single slice thick, yielding a sampling volume 3.4 mm deep in the z-axis, whereas those defined on the HR+ were 1–2 slices thick (2.4 to 4.8 mm deep). The same ROI set was applied to the baseline and post-AMPH images for each study, eliminating the possibility that rater-bias affected the comparisons. A single rater (WCD) defined all ROI.

The primary ROI were defined as follows: The dorsal caudate (DCA) was defined as the grey matter delimited anteromedially by the frontal horn of the lateral ventricle and posterolaterally by white matter in an image plane passing through the head and neck of the caudate nucleus (Figure 1). This plane corresponded to an image slice between the OM+17.5 and OM+20 (i.e., 17.5 and 20 mm, respectively, dorsal to the orbital-meatal plane) of the baboon brain in the atlas of Riche et al. (1988). The anteroventral striatum (AVS) was defined in an image slice approximating the OM+10 plane (i.e., 10 mm above the orbital-meatal plane) in the atlas of Riche et al. (1988) as the grey matter at the ventral lip of the anterior limb of the internal capsule (Heimer and Alheid 1991). This ROI was bounded anteriorly, medially, and laterally by white matter and posteriorly by a line drawn horizontally from the caudal border of the medial caudate. This ROI putatively included the accumbens, the ventromedial caudate, and the anteroventral putamen. The reference region for measuring the free and nonspecifically bound [¹¹C]raclopride was defined in the cerebellar cortex (Hall et al. 1994) in ventral image planes where the cortex was easily delimited from the cerebellar peduncles. This cerebellar ROI extended dorsally and posteriorly to no closer than 10 mm from the occipital cortex.

For *post hoc* assessments of the specificity of ΔBP differences between the DCA and the AVS, additional ROI were defined in other striatal regions. To ensure that differences in ΔBP between the DCA and AVS were not better accounted for by changes in the putamen, a dorsal putamen ROI was defined in the first image plane ventral to the plane containing the DCA-ROI as the grey matter bounded anteriorly and posteriorly by the anterior and posterior limbs of the internal capsule, respectively, and laterally by the external capsule (Figure 1). A ventral putamen ROI was drawn on the same horizontal plane as the anteroventral striatal ROI, bounded
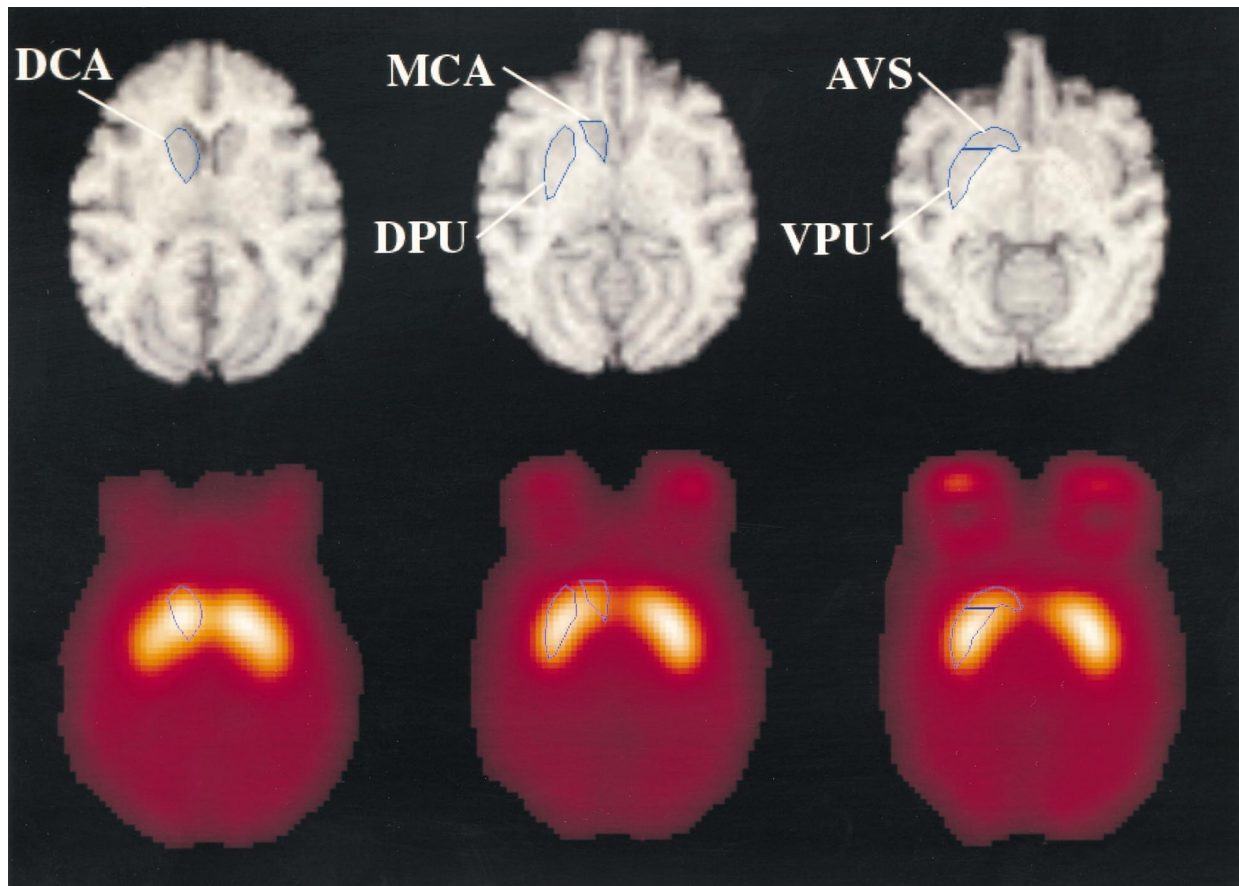
Figure 1. Co-registered PET (lower) and MRI (upper) sections through three levels of the striatum showing the ROI placement. The MRI image has been resliced into the same space and slice thickness as the PET image (Woods et al. 1993), and the ROI were defined on the MRI image and then used to measure the [^{11}C]raclopride binding in the coregistered PET image. The PET image shown is a parametric image of radiotracer distribution volume (DV; Logan method) and shows high radioactivity concentrations in the DA D2/D3 receptor rich striatum and relatively low radiotracer uptake in non-striatal areas (Hall et al 1994). The highest DV values were located in the putamen, and although the DA D2/D3 receptor Bmax is also highest in the putamen (Hall et al. 1994), physical aspects of the PET signal contribute likewise to this observation. Thus, while these images are aligned to sub-voxel accuracy, the curved geometry of the striatum, the spilling in of radioactive counts from slices above and below the ROI, and dilutional partial volume averaging effects all contribute to the spatial distribution of measured radioactive counts from the striatum, giving a slightly different appearance from that of the actual anatomy (e.g., in the slice through the dorsal caudate, the spilling in of radioactive counts from the putamen is evident) (Links et al. 1996; Mazziotta et al. 1981; Meltzer et al. in press). The relatively low DV in the AVS likely reflects both the lower concentration of DA D2/D3 receptors in the accumbens relative to the putamen (Hall et al. 1994) and the dilutional effects of being situated adjacent to areas with low receptor density (Links et al. 1996). The PET measures for each ROI included both left and right sided structures, but only the right-sided ROI are shown here so that the anatomy evident in the MRI will not be obscured by the ROI on one side. *Abbreviations*: AVS, anteroventral striatum; DCA, dorsal caudate; DPU, dorsal putamen; MCA, middle caudate; VPU, ventral putamen.

anteriorly by the posterior boundary of the AVS-ROI, medially by the pallidum, and laterally by the external capsule.

To ensure that differences between the DCA and the AVS were not better accounted for by AMPH-induced changes in caudate tissue located between these ROI, a middle caudate ROI was defined as the grey matter lateral to the lateral ventricles and anterior to the anterior limb of the internal capsule in an image plane that ap-

proximated level OM+15 of Riche et al. (1988). Because this middle caudate ROI was located within one FWHM of the DCA and the AVS, the middle caudate measures were not expected to be independent from those in the primary ROI, and were inspected *post hoc* to ensure that the true peak ΔBP was not located between the DCA and the AVS.

Decay-corrected, tissue time-radioactivity curves were generated for each ROI from the dynamic PET im-

age. A calibrated phantom standard was used to convert tomographic counts to μCi/ml of brain in each ROI for each time point. Since laterality effects were not hypothesized, the ROI from the left and right hemispheres were combined.

Data Analysis

Receptor availability as a function of AMPH-induced changes in endogenous [DA] was measured using a graphical analysis technique developed for assessing reversible radioligand-receptor interactions (Logan et al. 1990; Dewey et al. 1992). This Logan analysis provided a linear regression slope that was a measure of the total radioligand distribution volume (DV) (Logan et al. 1990). Regional DV values were used to calculate binding potentials (BP) (Mintun et al. 1984) to assess DA D2/D3 receptor specific binding. The BP was calculated as (Lammertsma et al. 1996):

$$BP = (DV_{ROI} - DV_{F+NS})/DV_{F+NS} =$$
$$(DV_{ROI}/DV_{F+NS}) - 1 = B'_{max}f_2/K_D$$

where B'_{max} (nM) is the concentration of available receptors, K_D (nM) the equilibrium dissociation constant, and f_2 the free fraction of radiotracer in brain (unbound in the precursor pool). The cerebellar data were used to determine the DV of free and nonspecific binding ($DV_F + NS$) under the assumptions that the specific binding of [11C]raclopride in the cerebellum was negligible and that the concentration of free and nonspecifically bound radioligand (F + NS) in the cerebellum approximated F + NS in all regions (Hall et al. 1994). AMPH binding to DA D2/D3 receptors is also negligible (Burt et al. 1976).

The AMPH-induced percent change in BP (ΔBP) for [11C]raclopride between the baseline ($BP_{baseline}$) and post-AMPH (BP_{AMPH}) scans was calculated as: [($BP_{AMPH} - BP_{baseline}$) / $BP_{baseline}$] $\times$ 100. The *a priori* hypothesis that ΔBP in the AVS exceeds that in the DCA was tested using a paired *t*-test. Because of the long time intervals between different studies performed within individual monkeys (Table 1), these measures were assumed to be independent in assigning degrees of freedom. In *post hoc* assessments, the ROI in the putamen was added to the primary ROI to examine main effects of region by ANOVA, with the significance of differences between regions assessed by the Tukey HSD test. The relationships between AMPH dose and regional [11C]raclopride binding in the AVS, the DCA and the putamen were assessed using Pearson product-moment correlation coefficients.

Simulation Studies of Error from Partial Volume Effects and Image Misregistration

Estimating the True Spatial Resolution of the Images. To simulate the effects of scanner resolution (also called partial volume) and inaccuracies in image coregistration on the regional ΔBP measures, we first estimated the true image resolution by considering the intrinsic scanner resolution, the broadening due to scatter, the broadening from image smoothing, and the image acquisition mode. The 951R studies were acquired in the 2D (plane-by-plane) mode, with septa extended into the field-of-view. For images acquired under these conditions the resolution of a point source *in air* reconstructed without smoothing is 6 $\pm$ 0.5 mm full-width at half-maximum (FWHM) in the transverse plane and 5 $\pm$ 1 mm FWHM axially (Spinks et al. 1992). During reconstruction, the effect of the Hanning window with cut-off = Nyquist frequency only slightly increased the transverse FWHM (i.e., by < 6%), and no axial smoothing was applied. Measurements of point sources in a *water* phantom indicated that for brain-sized objects the effect of scatter from tissue is an additional broadening of ~5mm FWHM added in quadrature to the transverse resolution (Meltzer et al. in press), whereas the average axial resolution is only slightly increased to 5.3 mm [probably due to the rejection of oblique scatter by the septa]. The combination of these effects resulted in a true image FWHM resolution estimate of 7.8 mm in the transverse plane and 5.3 mm axially for the 951R images.

The HR+ images were acquired in 3D (volume) mode with septa retracted. For images acquired under these conditions the FWHM resolution of a point source in air is approximately 5 $\pm$ 0.5 mm transverse and 4.5 $\pm$ 0.5 mm axially (Brix et al. 1997). The image reconstruction using a Hanning window with cut-off = Nyquist frequency resulted in an estimated (including the effect of scatter) true image FWHM resolution of 7.1 mm in the transverse plane and 6.7 mm axially (P. Kinahan, unpublished data). The broader axial resolution in this case arises from the lack of septa in the HR+ studies, resulting in a degradation of axial resolution by oblique scatter.

Our simulations therefore assumed a transverse FWHM resolution of 8 mm and an axial resolution of 6 mm. These assumptions comprised a slightly conservative estimate of resolution in the transverse direction and a compromise between the two scanners in the axial direction.

Generating a Reference Image for Simulation Studies. A 'ground truth' reference image was derived from a parametric image of [11C]raclopride DV (Figure 1) for one study (Baboon E; Table 1). A DV image was selected for the simulations because DV, in contrast to BP, is linearly related to the dynamic PET data, and thus equally affected by resolution effects. The impact of the changes in partial volume and alignment error applied to this reference image were assessed via the resulting changes in the derived BP values measured in each ROI (Figure 1).

The reference image was defined by segmenting the parametric DV image into two regions corresponding to the basal ganglia (specifically bound tracer) and the remainder of the brain. Since non-basal ganglia tissues have DA D2/D3 densities < 10% of that of the striatum, they were assumed to reflect non-specifically bound tracer (Hall et al. 1994). This simplification of DV in the remainder of the brain did not detract from the estimation of partial volume and misalignment effects on ΔBP, because the simulations were not intended to replicate the actual measured ΔBP (which is not feasible due to the number of free parameters involved in defining the reference image, image resolution, alignment accuracy, and non-specific tracer binding patterns in the pre- and post-AMPH images). The threshold DV for defining the edge of the striatum in the reference image was selected so that when this image was blurred to the spatial resolutions described above, the resulting image matched the original image of measured DV, except for having a more uniform appearance. The segmented basal ganglia were then subdivided into four bilateral regions corresponding to the ROI in the DCA, AVS, middle caudate, and putamen (Figure 1). The DV values of these four regions were manually adjusted so that the ROI placed on the blurred image reproduced (to within 3%) the measured DV values.

Simulating Partial Volume Effects on Regional ΔBP.
The post-AMPH DV image was defined by changing the DV for non-specific binding by the measured ΔDV of the cerebellum, and the DV of each basal ganglia region was systematically varied by additional increments as described below. The resulting post-AMPH images were blurred to the above-stated resolutions, and the ΔBP values for each ROI were calculated by comparing the simulated reference and post-AMPH images. To investigate the coupling between ΔBP for the DCA and the AVS, the DV values in the DCA, middle caudate, and putamen were reduced by 10% beyond that of the cerebellum, and the DV of the AVS was then sequentially decreased by 5% increments to 10–30% beyond the cerebellar ΔDV. In a similar manner the coupling between the AVS and putamen was studied by fixing the AVS ΔDV to a 20% decrement (the middle of the range tested above) relative to the cerebellar ΔDV and the putamen DV was sequentially reduced by 5% increments between 10 and 30%. The resulting estimated ΔBP values for the AVS and DCA were computed for each set of cases.

Simulating the Effects of Alignment Error on ΔBP.
Although the similarity in PET images allows excellent registration of pre- and post-AMPH images, the alignment of PET and MRI images is subject to small errors, shown by rigorous, invasive methods to have a mean absolute error of 1.62 mm for subcortical test points in baboons (Black et al. 1997), similar to that described for

humans (Woods et al. 1993). When coupled with the alignment verification strategy described above (Wiseman et al. 1996), the final registrations for the baboon studies considered herein were estimated by visual inspection to have maximum alignment error of less than the transverse dimension of one voxel, or ∼1.5 mm. Similarly, the maximum error in pitch (equivalent to head nodding) was < 4 degrees, which for the ROIs used in this case, corresponds to an axial shift of up to 1.7 mm. The ROI-based measures of ΔBP for the AVS and the DCA were obtained as the MRI-derived ROIs were shifted by ±1.5 mm in each of the left-right, anterior-posterior, and dorsal-ventral axes for the simulated case in which DV decreased by 10% in the DCA and the middle caudate, and by 20% in the AVS and the putamen in the post-AMPH relative to the reference image. From these values, the average error and the standard deviation of the ΔBP were calculated for the AVS and the DCA to assess the effects of misalignment between the PET image and the MRI-based ROI.

RESULTS

The HPLC analyses of the concentrations of [^{11}C]raclopride and radiolabelled metabolites showed that about 70% and 10–20% of [^{11}C]raclopride in plasma was unmetabolized at 10 min and 60–90 min, respectively. The metabolism of [^{11}C]raclopride did not significantly differ between the baseline and AMPH-treated conditions or across AMPH doses. Immediately after [^{11}C]raclopride infusion, radioactivity accumulated bilaterally in the striatum, reaching a peak value in ∼10 min and clearing to between 25% and 40% of the peak value at 60 min (Figure 2). Cerebellar radioactivity reached a peak within 5 min but cleared more rapidly, with ≤10% of the peak activity remaining at 60 min (Figure 2).

The mean volumes defined to sample the regional radioactivity concentration were similar across striatal ROI. The mean volumes in mm³ ± 1 SD were: AVS, 484 ± 145; DCA, 548 ± 67.3; middle caudate, 363 ± 131; dorsal putamen, 533 ± 191; and ventral putamen, 532 ± 157. The ROI for the 3D HR+ images were positioned 24.6 to 38.1 mm from the center of the axial FOV within the range where signal-to-noise is relatively uniform (Townsend et al. 1998). For the axially uniform 2D 951R images the ROI ranged from 0 to 16.9 mm (5 planes) from the axial FOV center.

The Logan graphical analyses were applied to data acquired from 5 to 60 min post-injection, with correlation coefficients (r^2) for the linear regression exceeding 0.99 for all ROI for all scans. The rank order of the mean baseline DV and BP values by region was highest in putamen, high in DCA, and slightly lower in AVS (Table 1; mean baseline cerebellar DV = 0.901 ± 0.198). This rank order was consistent across scans, as in all 12
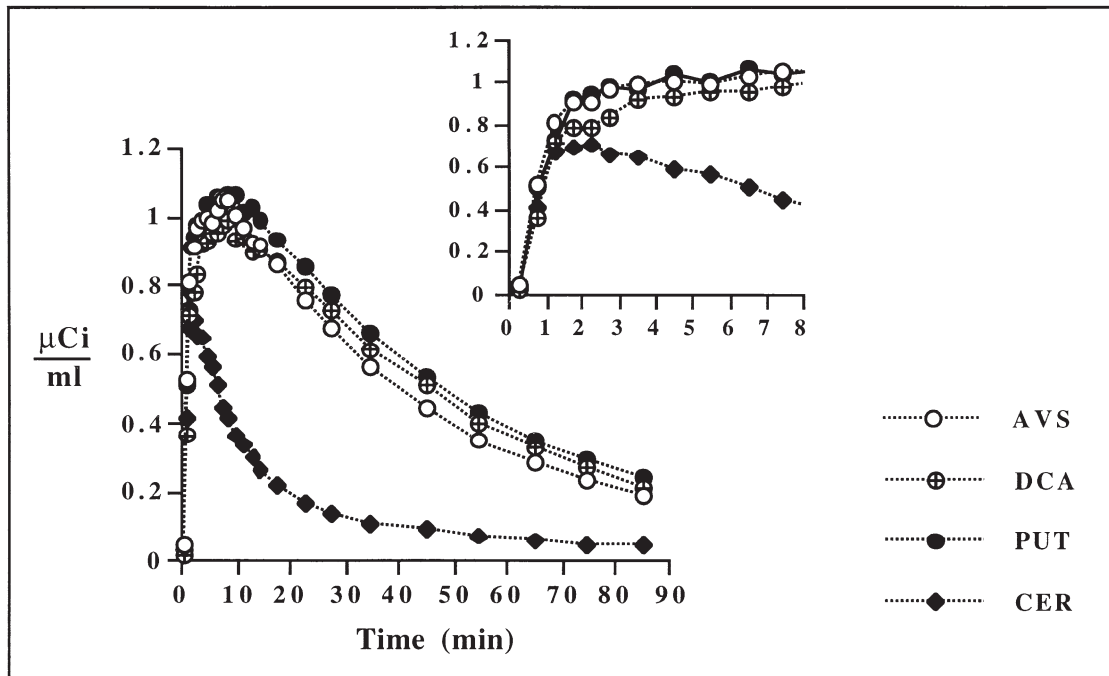
Figure 2. PET measures of the radioactivity concentration over 90 minutes in the putamen (PUT), the dorsal caudate (DCA), the anteroventral striatum (AVS), and the cerebellum (CER) measured using 3D PET after intravenous injection of high specific activity [^{11}C]raclopride (8 mCi) in baboon B (Table 1). The inset graph shows the early curve times from 0 to 8 min post-injection. Similar curves shapes are observed for all three striatal ROI (AVS, DCA, PUT), while lower uptake and rapid clearance is observed in the cerebellum.

baseline studies the AVS had a BP value lower than that in the DCA and putamen, and in 10 of 12 of these studies the BP in the putamen was higher than that of the DCA. The baseline BP measures and the AMPH-induced ΔBP values obtained using the HR+ scanner were within the range of those obtained using the 951R scanner.

The mean DV in the cerebellum did not significantly differ between the baseline and the post-AMPH conditions (mean DV increased 2.95% $\pm$ 11.0%; $t = 0.93$). In contrast, AMPH pretreatment reduced the BP in all 12 studies in the AVS (mean ΔBP $= -19.0\% \pm 9.1\%$ for all AMPH doses combined; paired $t = -7.23$; $p < .001$; $df = 11$) and in 11 of 12 studies in the DCA (mean ΔBP $= -9.56 \pm 11.6$; $t = -2.85$; $p < .01$). The magnitude of the mean reduction in BP in the AVS was 99.2 $\pm$ 79.6% greater than that in the DCA ($t = 4.32$; $p < .002$), confirming the *a priori* hypothesis (Figure 3). The magnitude of ΔBP in the AVS exceeded that in the DCA in 11 of 12 studies (Figure 4).

Post hoc assessments addressed the specificity of this difference in ΔBP between the DCA and the AVS and examined the relationship between AMPH dose and ΔBP (Table 1). The ΔBP in the middle caudate was lower in magnitude than that in the AVS in all 12 studies. The magnitude of the mean ΔBP in the AVS ($-19.0 \pm$
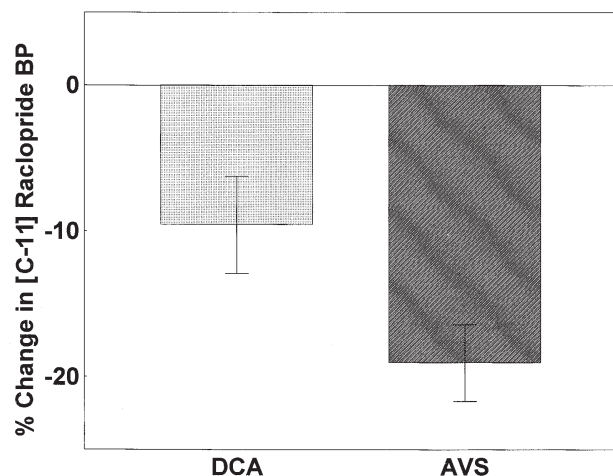

Figure 3. Mean changes in the binding potential (ΔBP) for [^{11}C]raclopride in the anteroventral striatum (AVS) and the dorsal caudate (DCA). The comparison between the ΔBP values for all AMPH doses combined comprises the test of the *a priori* hypothesis, and shows that the sensitivity to AMPH-induced DA release is higher in the AVS than the DCA ($p < .001$), consistent with the results of microdialysis studies performed in rats (e.g., Di Chiara et al. 1993).
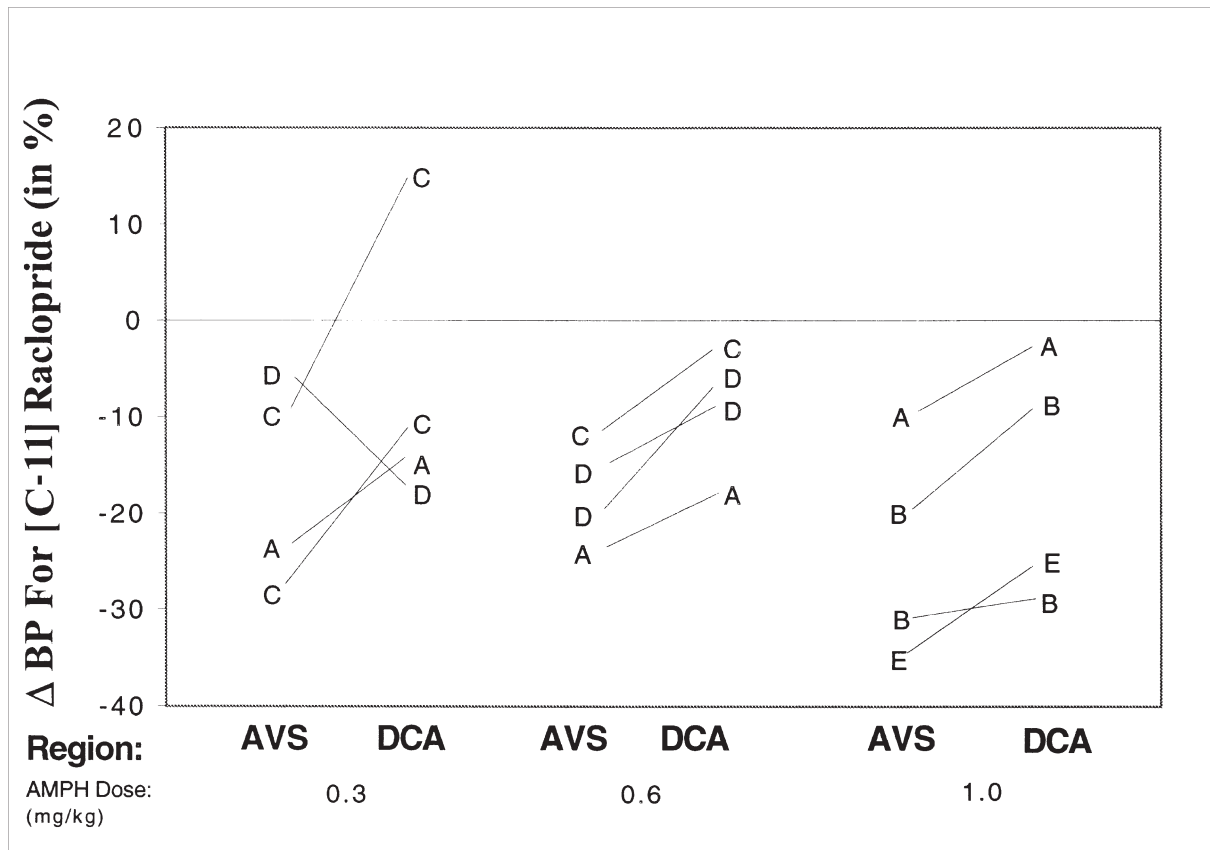
Figure 4. The ΔBP values obtained at individual AMPH doses showing the relationship between ΔBP in the anteroventral striatum (AVS) and the dorsal caudate (DCA) within individual studies. Each set of paired values is connected by a line. Although the ΔBP measured both within and across animals at a given AMPH dose is highly variable (as noted by previous studies), the larger magnitude of the ΔBP in the AVS as compared with the DCA is evident within studies at each AMPH dose administered. The letters show the identity of each baboon (see table 1).

9.1) was $61.2 \pm 28.6\%$ higher than that of the middle caudate $(-11.8 + 10.2\%)$ for all doses combined (paired $t = -7.42; p < .001$).

The dorsal and ventral putamen measures were highly correlated (Table 1), so were combined into a single ROI for the *post hoc* ANOVA and linear regression analyses. A significant main effect of region was evident by ANOVA ($F = 14.1, p < .001$), which was largely accounted for by the significantly greater mean ΔBP of [^{11}C]raclopride in both the AVS and the putamen relative to the DCA ($p < .0004$ and $p < .0006$, respectively, by Tukey's HSD test). The ΔBP did not significantly differ between the putamen and the AVS (mean $\Delta BP = -18.6 \pm 12.6$ and -19.0 ± 9.1, respectively, for all AMPH doses combined). The inverse correlation between AMPH dose and ΔBP was significant in the putamen ($r = -0.60, p < .05$) but not the DCA ($r = -0.42$) or the AVS ($r = -0.33$) (Table 1; Figures 4 and 5).

The results of the simulation studies of partial volume effects are illustrated in Figure 6. Both plots show that the DCA values were only slightly influenced by changes in the DV of the AVS (Figure 6A) or the putamen (Figure 6B). In contrast, varying the ΔDV of the

putamen more prominently affected the ΔBP of the AVS (Figure 6B). For example, changing the putamen ΔDV from -20% to -30% resulted in an absolute change in the AVS ΔBP of $\sim 2.5\%$) (Figure 6B).

The effects of alignment errors between the simulated PET images and the MR-based ROI showed that average changes in the ΔBP values of the AVS and the DCA of 8% for both regions, with standard deviations of 25% (AVS) and 34% (DCA). The largest changes were observed for shifts along the anterior-posterior axis.

DISCUSSION

These PET measures of AMPH-induced changes in DA D2/D3 receptor availability are consistent with the hypothesis that the magnitude of AMPH-induced DA release is greater in the AVS than the DCA in baboons. The magnitude of the reduction in [^{11}C]raclopride binding in baboons was two-fold higher in the AVS than the DCA (Figure 3), similar to the $\sim$2-fold higher AMPH-induced DA pulse in the accumbens relative to the dorsal striatum measured in rats by microdialysis (Di Chi-
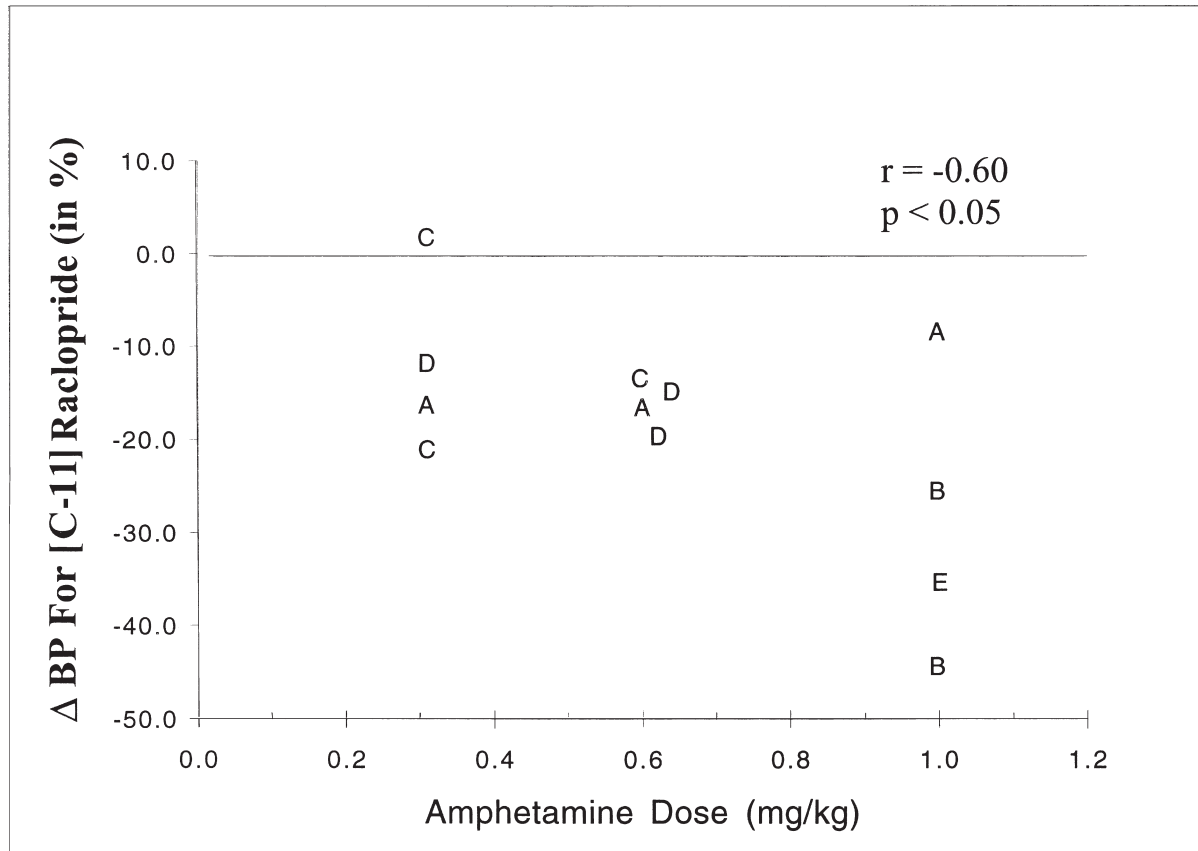
Figure 5. The percent change in the [^{11}C]raclopride binding potential (ΔBP) in the putamen at each AMPH dose. The alphabetical characters refer to the animals listed in Table 1 to permit correlations with the corresponding values in the AVS and the DCA shown in Figure 4. These data are consistent with the results of previous studies which showed that the relationship between ΔBP and AMPH dose is approximately linear through the range tested in ROI that predominantly sampled the putamen (e.g., Laruelle et al. 1997; Carson et al. 1997).

ara et al. 1993). The similar relative magnitude of these effects is noteworthy because the relationship between the [^{11}C]raclopride ΔBP and the integral of the AMPH-induced DA pulse appears linear over the AMPH doses tested (Endres et al. 1997; Laruelle et al. 1997). Confidence limits established by simulation studies showed the regional differences in mean ΔBP are robust to error from partial volume and image misalignment. These data suggest that the preferential sensitivity of the ventral striatum to the DA releasing effects of AMPH exists in primates as well as rats (Di Chiara and Imperato 1988b).

An unexpected finding of the *post hoc* analyses was that the magnitude of the AMPH-induced ΔBP was also greater in the putamen than the DCA. The amount of DA released in the putamen during AMPH administration had not been compared to that in the caudate or the accumbens in previous microdialysis or neuroimaging studies. We thus had no *a priori* hypothesis about the AMPH-induced ΔBP in the putamen relative to other striatal regions.

Previous neuroimaging studies have not compared changes in the specific binding parameter for DA receptor radioligands during pharmacological challenge across different striatal regions. Our ability to do so depended on the use of MRI-based ROI analysis, since borders between striatal areas are not evident in PET images (Figure 1), and the use of relatively high resolution PET tomographs which provided 5 to 8 image slices through the baboon striatum. In contrast, previous studies centered ROI directly over PET voxels showing the highest radioactivity concentration, a practice that emphasize the putamen (Figure 1) (Hall et al. 1994), and the reductions in DA receptor specific binding they reported are likely to be most comparable to our data in the putamen (Figure 5).

Study Limitations

In primates the cells with histochemical and connectional features of the accumbens shell are scattered through the ventromedial caudate and anteroventral
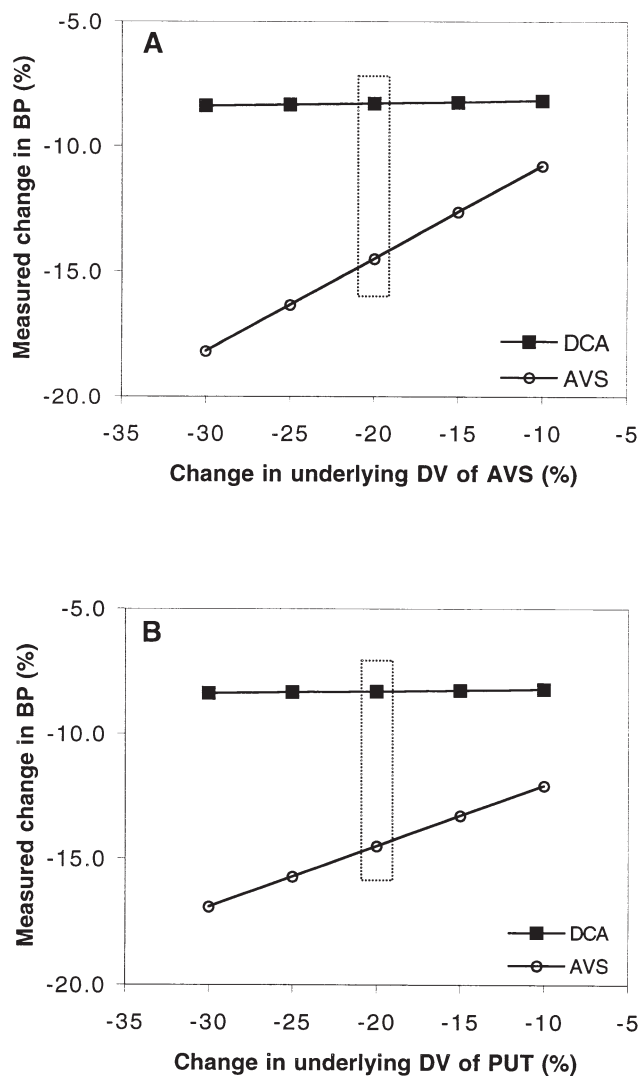
Figure 6. Relationships between the percent change in the ΔBP of the anteroventral striatum (AVS) and the dorsal caudate (DCA) in simulated PET images as tracer distribution volume (DV) of the AVS and the putamen are systematically varied. (A) Change in the ΔBP of the AVS and the DCA as the AVS ΔDV varies. (B) Change in the ΔBP of the AVS and the DCA as the putamen ΔDV varies. Common points between the two comparisons are shown in the dotted boxes (i.e., for the simulations shown in 6A, the putamen ΔDV is fixed at −20%, whereas in 6B the AVS ΔDV is fixed at −20%). In both simulations the ΔDV of the DCA remains fixed at −10%. The ΔDV values shown reflect additional changes above the change in free and nonspecific radiotracer binding, as measured in the cerebellum.

putamen (Alheid and Heimer 1988; Everitt et al. 1989; Heimer et al. 1991; Gerfen et al. 1985; Heimer and Alheid 1991). Neuroimaging studies are thus incapable of assessing whether the DA projections to the shell are

more sensitive to AMPH's DA-releasing effects than those to the rest of the AVS (Di Chiara et al. 1993).

A second limitation is that the baboons received ketamine and atropine 90 to 150 min prior to scanning. Both agents may increase DA release in the striatum through neurotransmitter system interactions, effects expected to subside prior to the baseline PET scan (Dewey et al. 1992; Smith et al. 1998a). If the elevated striatal DA concentrations induced by these agents persisted into this scan, however, the baseline BP and the AMPH-induced ΔBP measures would be attenuated. Differences in the magnitude of this effect across studies may have increased the variability of the PET measures. Moreover, since the DA-releasing effects of NMDA glutamate receptor antagonists such as ketamine are more robust in ventral than dorsal striatum (Carboni et al. 1989), these effects may have biased against finding an even more prominent differential AMPH-sensitivity in the AVS relative to the DCA.

Third, some scans were performed using relatively high injected doses of [^{11}C]raclopride (Table 1). The injected mass of raclopride in these studies, which averaged 10.5 ± 6.9 nmol (3.6 ± 2.4 μg) and ranged from 1.4 to 23.5 nmol (0.5 to 8.2 μg) may have resulted in significant DA D2/D3 receptor occupancy. The average equilibrium concentration of radiotracer in the striatum was 0.01% injected dose per gram, so the estimated striatal concentration of raclopride at equilibrium ranged from 0.14 to 2.4 nM. The density of DA D2/D3 receptor binding measured by [^{3}H]raclopride in the primate striatum averages ∼10 nM (Hall et al. 1994), so these raclopride concentrations may have occupied 1.4 to 24% of available receptors in the striatum. This effect would reduce the magnitude of apparent DV and BP values and contribute to the variability of these measures across scans. However, since raclopride binds equally to high and low affinity DA D2/D3 sites (see below) and the injected mass of raclopride was similar for the pre- and post-treatment scans, the ΔBP measures should not be differentially affected by the injected raclopride mass (AMPH promotes DA release via a mechanism independent of cell-firing, so the autoreceptor blockade resulting from this raclopride dose would not clearly affect the AMPH-induced DA pulse itself) (Kuczenski and Segal 1989). The data shown in Figure 4 indicate that the more prominent ΔBP in the AVS relative to the DCA is evident irrespective of whether a high or low injected mass of raclopride was used to acquire the PET images.

Fourth, it is conceivable that AMPH-induced cerebral blood flow (CBF) changes may have differentially affected tracer delivery across striatal regions. However, Hartvig et al. (1997) demonstrated similar AMPH-induced CBF changes across cortical and subcortical regions, suggesting that any difference in ΔCBF between the DCA and AVS would be subtle. Moreover, Logan et

al. (1994) showed that while large changes in CBF affect DV, the DV ratio (and hence the BP) is relatively insensitive to CBF changes. Finally, to assess differences in tracer delivery between regions or between pre- and post-AMPH conditions, we separately computed regional K1 values, which reflect tracer delivery, using compartmental modelling [this approach proved robust for both the pre- and post-AMPH images for 9 of the 12 scan-sets considered herein–methods described in Price et al. (1998)]. The mean baseline K1 values did not differ between the DCA and the AVS (0.17 ± 0.055 and 0.17 ± 0.040, respectively) and the mean AMPH-induced change in K1 was not significant in the AVS (0.0026 ± 0.053; $t = 0.15$) or the DCA (0.015 ± 0.038; $t = 1.16$).

Fifth, the PET results were sensitive to error from PET and MRI image misalignment. The simulated effects of misalignment between the PET data and the MRI-based ROI demonstrated that the sensitivity of the ΔBP was particularly high when misregistration occurred along the anterior-posterior axis. However, the misalignment errors for the actual studies appeared random, and the 99% difference between the mean ΔBP of the AVS relative to the DCA (Figure 3) was substantially greater than the 8% mean error from overall alignment inaccuracies obtained in the simulation studies.

Finally, the regional PET measures were affected by spilling in of radioactivity from surrounding tissues and dilutional effects from adjacent structures with low tracer uptake due to scanner resolution. Demonstrating a differential AMPH sensitivity for the AVS thus depended upon showing that the AMPH-induced change in [11C]raclopride binding was greater in the AVS than the DCA, and that this difference was not accounted for by an even greater change in the middle caudate or the posterior putamen. This approach was facilitated by the relatively low [11C]raclopride specific binding in extrastriatal areas, which reduced the number of comparisons required across regions (Hall et al. 1994) (Figure 1). The

ability of PET to resolve *relative differences* in the change in radiotracer concentration between two conditions in ROI separated by less than the FWHM resolution is central to PET's utility in localizing loci of maximal change in brain mapping studies (Fox et al. 1986).

To facilitate interpretation of the quantitative imaging results within the basal ganglia, simulation studies were performed to estimate the potential bias of partial volume effects and image misregistration error on ΔBP. These simulations showed that measured signals from the DCA and the AVS were easily differentiated, but that the AVS and putamen results were correlated (Figure 6). These results were consistent with the axial separation of ∼7.5 mm between the AVS and the DCA relative to the ∼6 mm axial resolution of the scanner, and the small anterior-posterior separation of the AVS and the putamen relative to the ∼8 mm transverse resolution. Nevertheless, Figure 6B shows that the putamen ΔDV must far exceed the AVS ΔDV before it can account for the ∼twofold difference in ΔBP found between the AVS and the DCA (Figure 3) on the basis of partial volume effects. Since the mean ΔDV of the putamen and the AVS were similar, the greater AMPH-induced ΔBP in the AVS relative to the DCA was not explained by partial volume effects from the putamen.

It is noteworthy that the data in Table 2 suggest the mean AVS ΔBP relative to the putamen ΔBP is larger at AMPH 0.3 mg/kg, similar at 0.6 mg/kg, and smaller at 1.0 mg/kg. Clear relationships between AMPH dose and ΔBP could not be established, since only four studies were obtained at each AMPH dose, each animal was not studied at each dose, and some animals were scanned using different PET cameras. These limitations did not detract from the test of the *a priori* hypothesis, because the preferential sensitivity to AMPH's DA releasing effects in the AVS relative to the DCA was demonstrated by paired comparisons within studies under various experimental conditions (Figure 4). Neverthe-

Table 2. Baseline Measures (Mean ± SD) of the Logan-Derived Distribution Volume (**DV**) and Binding Potential (**BP**) for [11C]raclopride in the Primary (bolded) and Secondary Regions-of-Interest (ROI). The Changes in the Specific Binding (ΔBP) of [11C]raclopride in the Post-AMPH Relative to the Baseline Scan are Expressed as the Mean % Change in BP (± one SD) at Each AMPH Dose Administered

		Regions-of-Interest				
		Primary ROI (Test of *a priori* Hypothesis)		Secondary ROI Assessed *post hoc*		
Kinetic Parameter	Sample Size (n)	Anteroventral Striatum	Dorsal Caudate	Mid-level Caudate	Dorsal Putamen	Ventral Putamen
Baseline **DV**	12	**2.28 (0.54)**	**2.69 (0.60)**	2.29 (0.56)	2.94 (0.61)	2.83 (0.58)
Baseline **BP**	12	**1.58 (0.56)**	**2.02 (0.45)**	1.55 (0.44)	2.30 (0.33)	2.19 (0.51)
ΔBP at 0.3 mg/kg	4	**−16.3 (10.8)**	**−4.45 (13.4)**	−8.53 (12.5)	−11.3 (10.7)	−11.2 (7.73)
ΔBP at 0.6 mg/kg	4	**−17.7 (4.86)**	**−8.37 (6.50)**	−13.3 (4.51)	−17.0 (3.13)	−16.6 (3.48)
ΔBP at 1.0 mg/kg	4	**−23.2 (11.3)**	**−15.9 (13.4)**	−13.6 (13.5)	−28.5 (12.5)	−28.9 (17.1)

less, the AMPH dose may prove salient to understanding potential differences in AMPH sensitivity between the AVS and the putamen.

Although the microdialysis data of DiChiara et al. (1993) showed the integral of the DA pulse increases nearly linearly as AMPH dose increases from 0.25 to 2.0 mg/kg in rats and the preferential release of DA in the accumbens shell relative to the dorsal caudate-putamen is equally robust for all AMPH doses in this range, the ability to detect such differences using PET is constrained by interactions between tracer and neurotransmitter kinetics that alter the apparent DA D2/D3 site affinity (Endres et al. 1997). The relationship between AMPH dose and DA release is demonstrable by PET at relatively low AMPH doses, but the sensitivity of ΔBP progressively diminishes at higher AMPH doses as the high affinity DA D2/D3 site occupancy increases (Endres et al. 1997; Hartvig et al. 1997). The DA D2/D3 receptor antagonist, raclopride, binds receptors in either the high or low affinity states, but competes with DA primarily at high affinity sites (Hartvig et al. 1997). Competition between DA and [^{11}C]raclopride at DA D2/D3 receptors in the low affinity state becomes a small factor only as DA concentrations enter the micromolar range ($K_D \sim 7.5$ nM and 4.3 μM for high and low affinity DA D2 receptor states, respectively) (Seeman et al. 1986).

The magnitude of the AMPH-induced ΔBP for [^{11}C]raclopride thus has an upper limit corresponding to the proportion of DA D2/D3 receptors in the high affinity state, reported from 30 to 90% (Richfield et al. 1986; Ross 1991; Seeman and Grigoriadis 1987; Sibley et al. 1982). Moreover, since some high affinity sites may be internalized, the true fraction of receptors available for competition may be lower since intracellular receptors are putatively more accessible to the lipophilic, [^{11}C]raclopride than to DA (Jin et al. 1998; Laruelle et al. 1997).

Consistent with this hypothesis, Hartvig et al. (1997) showed that in rhesus monkeys the relationship between ΔBP and AMPH dose (continuous i.v. infusion) was linear for AMPH plasma concentrations between 0 ng/ml and 5 ng/ml, but plateaued at $\sim -40\%$ as AMPH concentrations exceeded 10 ng/ml. Thus, mean reductions in DA D2/D3 receptor specific binding reported in PET and SPECT studies have not significantly exceeded 40% in response to various doses of AMPH (Carson et al. 1997; Dewey et al. 1993; Laruelle et al. 1997), methylphenidate (Volkow et al. 1994), GBR-12909 (Dewey et al. 1993), or cocaine (Schlaepfer et al. 1997). Although plasma AMPH concentrations were not reported by other neuroimaging studies for comparison with Hartvig et al. (1997), the dose range where ΔBP increases linearly with AMPH dose (i.v. bolus) appears to be up to a maximum of 0.4 to 1.0 mg/kg (Endres et al. 1997; Laruelle et al. 1997). Microdialysis stud-

ies show that AMPH doses in this range yield extracellular DA concentrations likely to saturate high-affinity DA D2/D3 sites. In monkeys, Endres et al. (1997) found that AMPH increased extracellular DA concentrations by up to 1100% at 0.2 mg/kg and 2500% at 0.4 mg/kg (to 839 nM), and Laruelle et al. (1997) showed that AMPH doses of 0.27, 0.68, and 1.0 mg/kg increased DA levels by 549, 1300, and 1600%, respectively, with the DA concentration at AMPH 0.5 mg/kg reaching 522 ± 205 nM. Since the mean DA D2/D3 receptor Bmax measured using [^{3}H]raclopride varies in primates from 8 fmol/mg of tissue in accumbens to 10 fmol/mg and 12 fmol/mg in caudate head and lateral putamen, respectively (Hall et al. 1994), extracellular DA concentrations of this magnitude would saturate the high affinity DA D2/D3 sites. The regional differences in Bmax also imply that these sites would saturate at lower AMPH doses in the accumbens than the lateral putamen. Thus if DA projections in accumbens are more sensitive to AMPH than those in putamen, PET would demonstrate this difference at low but not high AMPH doses, compatible with the trend in Table 2.

Possible Mechanisms for Regional Differences in Amphetamine Sensitivity

Although it remains unclear why DA projections would be more sensitive to AMPH's DA-releasing effects in the ventral than the dorsal striatum, this contrast may relate to regional differences in basal DA concentration. In rats the basal extracellular fluid DA concentration is 60 to 70% higher in the dorsal caudate-putamen than the accumbens, possibly due to the relatively higher density of DA neuron terminals in dorsal striatum (DiChiara et al. 1993). As basal DA concentrations increase and occupy more of the high affinity DA sites, the AMPH-induced DA pulse will displace less raclopride because more of the remaining receptors are in the low affinity state, reducing the apparent DA D2/D3 site affinity. Endres et al. (1997) estimated that a 20% increase in the basal DA concentration would attenuate the AMPH-induced ΔBP for [^{11}C]raclopride by 6.4%. If the basal DA concentration in the dorsal striatum exceeds that in the ventral striatum in primates, this effect may contribute to the difference in AMPH-induced ΔBP between these regions.

Since the effect of basal DA concentration on apparent site affinity is not a factor in microdialysis studies, other mechanisms must also play roles in the differential AMPH sensitivity between the dorsal and ventral striata. Weiss et al. (1992) showed an inverse correlation between basal DA concentration and DA release during cocaine challenge, and hypothesized this relationship indicated more potent activation of compensatory mechanisms to reduce DA neuron firing activity in areas with higher basal DA levels (we are unaware of

similar data assessing this relationship during AMPH-challenge). The higher DA neuron terminal density in the dorsal striatum may thus result in both higher basal DA concentrations and more efficient release modulation relative to the ventral striatum.

Implications for Human Studies

Neuroimaging studies of healthy humans have employed AMPH doses of 0.2 to 0.3 mg/kg and reported mean reductions in [^{11}C]raclopride BP of 15.5 ± 1.8% (Breier et al. 1997) and in [^{123}I]IBZM binding of 7.6 + 2.1% (Laruelle et al. 1996) when measured over the putamen or the entire striatum. Our results suggest the sensitivity for detecting AMPH-induced changes in DA receptor radioligand BP may be enhanced by measuring over the AVS. This difference may obtain for imaging studies involving other drugs of abuse as well, since cocaine, phencyclidine, narcotic analgesics, ethanol, and nicotine also preferentially increase extracellular DA in the accumbens in rats (Carboni et al. 1989; Di Chiara and Imperato 1988a; Imperato and Di Chiara 1986; Imperato et al. 1986; Brazell et al. 1990; Kuczenski and Segal 1992; Segal and Kuczenski 1992). Finally, it is noteworthy that the cognitive-behavioral challenge of Koepp et al. (1998), which involved playing a video game for monetary reward, reduced [^{11}C]raclopride BP more prominently in ventral than dorsal striatum. These data, which may reflect activation of DA projections into the ventral striatum by incentive-related processing, exemplify the importance of distinguishing DA release in specific striatal systems.

In primates the anteroventral and dorsal striata comprise major targets of the mesolimbic and mesostriatal subdivisions of the telencephalic DA system, respectively. The data presented here underscore the utility of functional imaging measures of endogenous DA release in investigations of mesolimbic DA function. Probing the function of this system is relevant to studies aimed at elucidating the neurobiological correlates of several psychopathological conditions, including depression, mania, psychosis, and substance abuse.

REFERENCES

Alheid GF, Heimer L (1988): New perspectives in basal forebrain organization of special relevance for neuropsychiatric disorders: The striatopallidal, amygdaloid, and corticopetal components of substantia innominata. Neuroscience 27:1–39

Black KJ, Gado MH, Videen TO, Perlmutter JS (1997): Baboon basal ganglia stereotaxy using internal MRI landmarks: Validation and application to PET imaging. J Comput Assist Tomogr 21 (6):881–886

Brazell MP, Mitchell SN, Joseph MH, Gray JA (1990): Acute administration of nicotine increases the in vivo extracellular levels of DA, 3,4-dihydroxyphenylacetic acid and ascorbic acid preferentially in the nucleus accumbens of the rat: Comparison with caudate-putamen. Neuropsychopharmacology 29:1177–1185

Breier A, Saunders R, Carson RE, Kolachana BS, de Bartolomeis A, Weinberger DR, Weisenfeld N, Malhotra AK, Eckelman WC, Pickar D (1997): Schizophrenia is associated with elevated amphetamine-induced synaptic dopamine concentrations: Evidence from a novel positron emission tomography method. Proc Natl Acad Sci USA 94:2569–2574

Brix G, Zaers J, Adam L-E, Belleman ME, Ostertag H, Trojan H, Haberkorm U, Doll J, Oberdofer F, Lorenz WJ (1997): Performance evaluation of a whole-body PET scanner using the NEMA protocol. J Nuc Med 38:1614–1623

Burt DR, Creese I, Snyder SS (1976): Properties of [^{3}H]haloperidol and [^{3}H]dopamine binding associated with dopamine release in calf brain membranes. Mol Pharmacol 12:800–812

Carboni E, Imperato A, Perezzani L, Di Chiara G (1989): Amphetamine, cocaine, phencyclidine, and nomifensine increase extracellular DA concentrations preferentially in nucleus accumbens of freely moving rats. Neurosceince 28:653–661

Carson RE, Breier A, de Bartolomeis A, Saunders R, Su TP, Schmall B, Der MG, Pickar D, Eckelman WC (1997): Quantification of amphetamine-induced changes in [^{11}C]raclopride binding with continuous infusion. J Cereb Blood Flow Metab 17:437–447

Deutch AY (1993): Prefrontal cortical dopamine systems and the elaboration of functional corticostriatal circuits: Implications for schizophrenia and Parkinson's disease. J Neural Transm 91:197–221

Dewey SL, Smith GS, Logan J, Brodie JD, Ding WY, Ferrieri RA, King PT, MacGregor RR, Martin TP, Wolf AP, Volkow ND, Fowler JS, Meller E (1992): GABAergic inhibition of endogenous dopamine release measured in vivo with ^{11}C-raclopride and positron emission tomography. J Neurosci 12(10):3773–3780

Dewey SL, Smith GS, Logan J, Brodie JD, Fowler JS, Wolf AP (1993): Striatal binding of the PET ligand ^{11}C-raclopride is altered by drugs that modify synaptic dopamine levels. Synapse 13:350–356

Di Chiara G (1991): On the preferential release of mesolimbic dopamine by amphetamine. Neuropsychopharmacology 5:243–244

Di Chiara G, Imperato A (1988a): Drugs abused by humans preferentially increase synaptic dopamine concentrations in the mesolimbic system of freely moving rats. Proc Natl Acad Sci USA 85:5274–5278

Di Chiara G, Imperato A (1988b): Opposite effects of μ and κ-opiate agonists on dopamine release in the nucleus accumbens and in the dorsal caudate of freely moving rats. J Pharmacol Exp Ther 244:1067–1080

Di Chiara G, Tanda G, Frau R, Carboni E (1993): On the preferential release of dopamine in the nucleus accumbens by amphetamine: further evidence obtained by vertically implanted concentric dialysis probes. Psychopharmacology 112:398–402

Endres CJ, Kolachana BS, Saunders RC, Su T, Weinberger D, Breier A, Eckelman WC, Carson RE (1997): Kinetic modeling of [^{11}C]raclopride: Combined PET-Microdialysis studies. J Cereb Blood Flow Metab 17:932–942

Everitt BJ, Cador M, Robbins TW (1989): Interactions between the amygdala and ventral striatum in stimulus-reward associations: Studies using a second-order schedule of sexual reinforcement. Neuroscience 30:63–75

Fibiger HC (1991): The dopamine hypotheses of schizophrenia and mood disorders. In Willner P, Scheel-Kruger J (eds), The Mesolimbic Dopamine System: From Motivation to Action. New York, Wiley, pp 615–638

Fox PT, Mintun MA, Raichle ME, Miezin FM, Allman JM, Van Essen DC (1986): Mapping human visual cortex with positron emission tomography. Nature 30:806–809

Gerfen CR, Baimbridge KJ, Miller JJ (1985): The neostriatal mosaic: Compartmental distribution of calcium-binding protein and parvalbumin in the basal ganglia of the rat and monkey. Proc Natl Acad Sci USA 82:8780–8784

Grace AA (1991): Phasic versus tonic dopamine release and the modulation of dopamine system responsivity: A hypothesis for the etiology of schizophrenia. Neuroscience 41:1–24

Hall H, Sedvall G, Magnusson O, Kopp J, Halldin C, Farde L (1994): Distribution of D_1- and D_2-dopamine receptors, and dopamine and its metabolites in the human brain. Neuropsychopharmacology 11:245–256

Halldin C, Farde L, Högberg T, Hall H, Ström P, Ohlberger A, Solin O (1991): A comparative PET study of five carbon-11 or fluorine-18 labelled salicylamides. Preparation and in vitro dopamine D-2 receptor binding. Nucl Med Biol 18:871–881

Hartvig P, Torstenson R, Tedroff J, Watanabe Y, Fasth KJ, Bjurling P, Långström B (1997): Amphetamine effects on dopamine release and synthesis rate studied in the Rhesus monkey brain by positron emission tomography. J Neural Transm 104:329–339

Heimer L, Zahm DS, Churchill L, Kalivas PW, Wohltmann C (1991): Specificity in the projection patterns of accumbal core and shell in the rat. Neuroscience 41:89–125

Heimer L, Alheid GF (1991): Piecing together the puzzle of basal forebrain anatomy. In Napier TC, Kalivas PW, Hanin I (eds), The Basal Forebrain. New York, Plenum Press, pp 1–42

Imperato A, Di Chiara G (1986): Preferential stimulation of dopamine-release in the nucleus accumbens of freely moving rats by ethanol. J Pharmacol Exp Ther 239:219–228

Imperato A, Mulas A, Di Chiara G (1986): Nicotine preferentially stimulates dopamine release in the limbic system of freely moving rats. Eur J Pharmacol 132:337–338

Jin H, George SR, O'Dowd BF (1998): The significance of the CDC2 phosphorylation site in agonist-induced D1 dopamine receptor internalization. Soc Neurosci Abstr 24:598

Johnson LA, Pearlman G, Miller CA, Young TI, Thulborn KR (1993): MR quantification of cerebral ventricular volume using a semiautomated algorithm. AJNR 14:1373–1378

Koepp MJ, Gunn RN, Lawrence AD, Cunningham VJ,

Gagher A, Jones T, Brooks DJ, Bench CJ, Grasby PM (1998): Evidence for striatal dopamine release during a video game. Nature 393:266–268

Kohler C, Hall H, Ogren SO, Gawell L (1985): Specific in vitro binding and in vivo binding of the [^{3}H] Raclopride: A potent substituted benzamide drug with high affinity for dopamine D-2 receptors in the rat brain. Biochem Pharmacol 34:2251–2259

Kuczenski R, Segal D (1992): Differential effects of amphetamine and DA uptake blockers (cocaine, nomifensine) on caudate and accumbens dialysate DA and 3-methoxytyramine. J Pharmacol Exp Ther 239:219–228

Kuczenski R, Segal D (1989): Concomitant characterization of behavioral and striatal neurotransmitter response to amphetamine using in vivo microdialysis. J Neurosci 9(6):2051–2065

Lammertsma AA, Bench CJ, Hume SP, Osman S, Gunn K, Brooks DJ, Frackowiak RSJ (1996): Comparison of methods for analysis of clinical [^{11}C]raclopride studies. J Cereb Blood Flow Metab 16(1):42–52

Laruelle M, Abi-Dargham A, Gil R, vanDyck CH, D'Souza D, Rosenblatt W, Kruger S, McCance-Katz E, Brenner L, Zea-Ponce Y, Zoghbi SS, Abi-Saab D, Fingado C, Baldwin RM, Hoffer PB, Krystal J, Charney DS, Innis RB (1996): Single photon emission computerized tomography imaging of amphetamine-induced dopamine release in drug free schizophrenic subjects. Proc Natl Acad Sci USA 93:9235–9240

Laruelle M, Iyer RN, Al-Tikriti MS, Zea-Ponce Y, Malison R, Zoghbi SS, Baldwin RM, Kung HF, Charney DS, Hoffer PB, Innis RB, Bradberry CW (1997): Microdialysis and SPECT measurements of amphetamine-induced dopamine release in nonhuman primates. Synapse 25:1–14

Links JM, Zubieta JK, Meltzer CC, Stumpf MJ, Frost JJ (1996): Influence of spatially heterogenous background activity on "hot object" quantitation in brain emission computed tomography. J Comput Assist Tomogr 20(4):680–687

Logan J, Fowler JS, Volkow ND, Wolf AP, Dewey Sl, Schlyer D, MacGregor R, Hitzemann R, Bendriem B, Gatley SJ, Christman DR (1990): Graphical analysis of reversible radioligand binding from time activity measurements applied to [N-^{11}C-methyl]-(-)-cocaine PET studies in human subjects. J Cereb Blood Flow Metab 10:740–747

Logan J, Volkow ND, Fowler JS, Wang G-J, Dewey Sl, MacGregor R, Schlyer D, Gatley SJ, Pappas N, King P, Hitzemann R, Vitkin S (1994): Effects of blood flow on [11C]raclopride binding in the brain: Model simulations and kinetic analysis of PET data. J Cereb Blood Flow Metab 14:995–1010

Mazziotta JC, Phelps ME, Plummer D, Kuhl DE (1981): Quantitation in positron emission computed tomography. 5. Physical-anatomical effects. J Comput Assist Tomogr 5:734–743

Meltzer CC, Kinahan PE, Greer PJ, Nichols TE, Comtat C, Cantwell MN, Lin MP, Price JC. Comparative evaluation of MR-based partial volume correction schemes for PET. J Nucl Med, in press

Minoshima S, Berger KL, Lee KS, Mintun MA (1992): An automated method for rotational correction and center-

ing of three-dimensional functional brain images. J Nucl Med 33(8):1579–1585

Mintun MA, Raichle ME, Kilbourn MR, Wooten GR, Welch MJ (1984): A quantitative model for the in vivo assessment of drug binding sites with positron emission tomography. Ann Neurol 15:217–227

Pehek EA, Schechter MD, Yamamoto BK (1990): Effects of cathinone and amphetamine on the neurochemistry of of dopamine in vivo. Neuropharmacology 29:1171–1176

Price JC, Mason NS, Lopresti B, Holt D, Simpson NR, Drevets W, Smith GS, Mathis CA (1998): PET measurement of endogenous neurotransmitter activity using high and low affinity radiotracers. In Carson R, Daube-Witherspoon M, Herscovitch P (eds), Quantitative Functional Brain Imaging with Positron Emission Tomography. San Diego, Academic Press, pp 441–448

Riche D, Hantraye P, Guibert B, Naquet R, Loc'h C, Maziere B, Maziere M (1988): Anatomical atlas of the baboon's brain in the orbito-meatal plane used in experimental positron emission tomography. Brain Res Bull 20:283–301

Richfield EK, Young AB, Penny JB (1986): Properties of D2 dopamine receptor autoradiography: High percentage of high-affinity agonist sites and increased nucleotide sensitivity in tissue sections. Brain Res 383:121–128

Robinson TE, Camp DM (1990): Does amphetamine preferentially increase the extracellular concentration of dopamine in the mesolimbic system of freely moving rats? Neuropsychopharmacology 3:163–173

Robinson TE, Kolb B (1997): Persistent structural modifications in nucleus accumbens and prefrontal cortex neurons produced by previous experience with amphetamine. J Neurosci 17(21):8491–8497

Ross SB (1991): Synaptic concentration of dopamine in the mouse striatum in relationship to the kinetic properties of the dopamine receptors and uptake mechanism. J Neurochem 56:22–29

Schlaepfer TE, Pearlson GD, Wong DF, Marenco S, Dannals RF (1997): PET study of competition between intravenous cocaine and [^{11}C]raclopride at dopamine receptors in human subjects. Am J Psychiatry 154:1209–1213

Seeman P, Guan H, Niznik C (1989): Endogenous DA lowers the dopamine D2 receptor density as measured by [^{3}H]raclopride: Implications for PET of the human brain. Synapse 3:96–97

Seeman P, Grigoriadis D (1987): Dopamine receptors in brain and periphery. Neurochem Int 10:1–25

Seeman P, Watanabe M, Grigoriadis D, Tedesco JL, George SR, Svensson U, Nilsson JLG, Neumeyer JL (1986): Dopamine D2 receptor binding sites for agonists. A tetrahedral model. Mol Pharmacol 28:391–399

Segal DS, Kuczenski R (1992): Repeated cocaine administration induces behavioral sensitization and corresponding decreased extracellular dopamine responses in caudate and accumbens. Brain Res 577:351–355

Sharp T, Zetterstrom T, Ljungberg, Ungerstedt U (1987): A direct comparison of amphetamine-induced behaviours

and regional brain dopamine release in the rat using intracerebral dialysis. Brain Res 401:322–330

Sibley DR, De Lean A, Creese I (1982): Anterior pituitary receptors: demonstration of interconvertible high and low affinity states of the D2 dopamine receptor. J Biol Chem 257:6351–6361

Smith GS, Schloesser R, Brodie JD, Dewey SL, Logan J, Vitkun SA, Simkowitz P, Hurley A, Cooper T, Volkow ND, Cancro R (1998a): Glutamate modulation of dopamine measured in vivo with positron emission tomography (PET) and ^{11}C-raclopride in normal human subjects. Neuropsychopharmacology 18:18–25

Smith GS, Price JC, Lopresti BJ, Huang Y, Simpson N, Holt D, Mason NS, Meltzer CC, Sweet R, Nichols T, Sashin D, Mathis CA (1998b): Test-retest variability of serotonin 5HT2A receptor binding measured with positron emission tomography and [^{18}F]altanserin in the human brain. Synapse 30:380–392

Spinks TJ, Jones T, Bailey DL, Townsend DW, Grootoonk S, Bloomfield PM, Gilardi MC, Casey ME, Sipe B, Reed J (1992): Physical performance of a positron tomograph for brain imaging with retractable septa. Physics Med Biol 37:1637–1655

Swerdlow NR, Koob GF (1987): Dopamine, schizophrenia, mania, and depression: toward a unified hypothesis of cortico-striato-pallido-thalamic function. Behav Brain Sci 10:197–245

Townsend DW, Isoardi RA, Bendriem B (1998): Volume imaging tomographs. In Bendriem B, Townsend DW (eds), The Theory and Practice of 3D PET. Boston, Kluwer Academic Publishers, pp 133–167

Volkow ND, Wang G-J, Fowler JS, Logan J, Schlyer D, Hitzemann R, Lieberman J, Angrist B, Pappas N, MacGregor R, Burr G, Cooper T, Wolf AP (1994): Imaging endogenous dopamine competition with [^{11}C]raclopride in the human brain. Synapse 16:255–262

Weiss F, Paulus MP, Lorang MT, Koob GF (1992): Increases in extracellular dopamine in the nucleus accumbens by cocaine are inversely related to basal levels: effects of acute and repeated administration. J Neurosci 12(11): 4372–4380

Willner P (1995): Dopaminergic mechanisms in depression and mania. In Bloom FE, Kupfer DJ (eds), Psychopharmacology: The Fourth Generation of Progress. New York, Raven Press, pp 921–932

Willner P, Ahlenius S, Muscat R, Scheel-Kruger J (1991): The mesolimbic dopamine system. In Willner P, Scheel-Kruger J (eds), The Mesolimbic Dopamine System: From Motivation to Action. New York, Wiley, pp 615–638

Wiseman M, Nichols T, Dachille M, Mintun M (1996): Working towards an automatic and accurate method for PET-MRI alignment. J Nucl Med 37 (5):224P

Woods RP, Masotho J, Cherry SR (1993): MRI-PET registration with automated algorithm. J Comput Assist Tomogr 17:536–546